AIAA AVIATION Forum
13-17 June 2016, Washington, D.C.
16th AIAA Aviation Technology, Integration, and Operations Conference

10.2514/6.2016-4363

Uncertainty Analysis for Calculating Reverse Thrust Using In Situ Data

Angela Campbell, Ph.D.[1] and Andrew Cheng, Ph.D.[2]
Federal Aviation Administration[3], Atlantic City International Airport, NJ, 08405

Runway excursions, abnormal runway contact, and runway undershoot/overshoot are the third leading category of fatal commercial aviation accidents. One contributing factor is the lack of timely objective and accurate assessments of runway conditions. Feasible methods of using onboard aircraft data to achieve a timely reporting of the available runway friction have been sought to improve real-time assessment of runway conditions. Though the aircraft braking capability is an essential element for the runway condition assessement, it is not directly measured. Critical forces acting on the aircraft during the landing rollout must be properly measured or estimated to enable the airplane-based reporting approach. The uncertainty of each force calculation will determine the validity of such approach.

In this study, we demonstrated a process to determine the uncertainty in the calculation of reverse thrust using in situ data. The analysis was performed on a reverser thrust model that uses a control volume analysis and engine station pressure and temperature ratios to calculate reverse thrust. The model was verified and validated using data collected by the FAA's Global 5000 aircraft. A sensitivity analysis was performed using a response surface methodology to determine the most critical factors in the analysis. Then a Monte Carlo simulation was used to determine the uncertainty in the response. The analysis found that the uncertainty in the model input variables translates to an uncertainty of ±10% for the reverse thrust calculation.

Nomenclature

$\dot{m}$	=	Mass flow rate
δ_S	=	Spoiler deflection angle
$\emptyset$	=	Relative humidity
a	=	Ambient
AR	=	Aspect ratio
b	=	Wing span
b_s	=	Spoiler span
B	=	Bypass
c	=	Combustor
C_D	=	Drag coefficient
C_{D0}	=	Zero-lift drag coefficient
C_{Dhld}	=	High lift device drag
C_{Ds}	=	Spoiler drag coefficient
C_L	=	Lift coefficient
C_{LC}	=	Clean wing lift coefficient
C_{LHLD}	=	High lift device lift coefficient
C_{LS}	=	Spoiler lift coefficient
d	=	Diffuser
D	=	Drag
e	=	Oswald efficiency
e	=	Exit
F	=	Force
G	=	Gravity
M	=	Mach

[1] Aerospace Engineer, Aviation Research Division, FAA WJHTC ANG-E272, and AIAA Member
[2] General Engineer, Aviation Research Division, FAA WJHTC ANG-E272
[3] The findings and conclusions in this paper are those of the author(s) and do not necessarily represent the views of the FAA.

m = Mass
η = Efficiency
N = Normal distribution
n = Nozzle
o = Inlet
p = Pressure
R = Gas constant
S = Wing area
sat = Saturation
S_s = Spoiler area
T = Temperature
t = Time
TR = Thrust reverser
U = Uniform distribution
u = Velocity
v = Vapor
V = Velocity
β = Ejection angle
γ = Specific heat ratio
ρ = Density

I. Introduction

Runway excursions while landing on contaminated runways is a continuing problem. A study by Boeing concluded that runway excursions, abnormal runway contact, and runway undershoot/overshoot were the third leading cause of fatal commercial aviation accidents between 2005 and 2014[1]. Furthermore, a study by the Flight Safety Foundation in 2009 showed that ineffective braking caused by runway contamination is the third leading cause of runway excursion events[2]. One contributing factor is a lack of timely, objective, and accurate information on runway friction. The National Transportation Safety Board (NTSB) has issued a number of safety recommendations since 1974 on the subject of runway friction determination in slippery runway conditions. As a result of the Southwest Airlines flight 1248 landing overrun at Chicago Midway airport on December 8, 2005, the NTSB recommended that the FAA should investigate the feasibility of using onboard aircraft data to achieve a timely assessment of the available runway friction[3].

The current methods of assessing runway conditions are pilot braking action reports and the use of continuous friction measuring equipment (CFME). Pilot braking action reports are useful in characterizing changing runway conditions; however, they are subjective and can vary widely between pilots and aircraft types. CFMEs are currently the source of objective runway friction assessments; however, they have their drawbacks, including lack of accuracy and repeatability. Furthermore, CFMEs do not directly address the braking performance of an aircraft. In addition, their use requires a temporary closure of a runway, which interrupts airport operations.

Given the limitations of current runway assessment methods, a novel approach has been proposed to determine runway friction by using aircraft onboard data during the landing roll-out[4]. During the landing roll-out, five primary forces are acting on the aircraft: thrust, drag, lift, gravity, and braking. Though the overall acceleration of the aircraft is always captured, the individual forces are not readily recorded in the aircraft data output. Regardless, drag, lift, and thrust can be estimated using an aircraft performance model and recorded flight parameters (e.g., airspeed, N1, longitudinal acceleration, and ground speed). The effect of gravity on the longitudinal acceleration of the aircraft can be estimated based on the slope of the runway. A direct estimate of braking force is not possible because data of braking torque or effective braking pressure are unavailable; however, it can be determined by balancing the forces acting on the aircraft given that adequeate estimates of the other forces are available.

Accurate information of braking force is essential to enable effective assessment of runway slipperiness. Because the braking force can only be calculated by estimating the other four forces acting on the aircraft and subtracting those values from the overall inertial data, its accuracy depends on the uncertainty of the calculation of the other forces. In this study, we demonstrated an analysis process to determine the uncertainty in the calculation of reverse thrust. The importance of the reverse thrust is twofold: (1) it has a significant effect on the aircraft deceleration rate and landing distance when being utilized, and (2) its calculation presents a complex challenge because of the large number of environmental, aircraft configuration, and engine design factors that impact the response. Because of the large number of aircraft types and variety of operating conditions encountered in the U.S.

commercial fleet, the data required for the reverse thrust calculation may be incomplete or at a low level of accuracy. That is, proprietary data for specific aircraft/engine design is not available and only estimates for the class of aircraft or engine can be found.

The first step in the uncertainty analysis process was to construct a reverse thrust model to ascertain the sensitivity of reverse thrust to a number of environmental, aircraft configuration, and engine design variables and to analyze the uncertainty in the calculation. The factors that have the greatest influence on the generated reverse thrust were identified and the accuracy of the information available in the public domain was evaluated. Finally, the expected error in the reverse thrust calculation and its effect on aircraft stopping distance were assessed.

This paper is organized into five subsequent sections. Section II describes the thrust reverser model used for the analysis. Section III discusses model verification and validation. Section IV describes the sensitivity analysis performed to determine which variables drive the reverse thrust response. Section V describes the uncertainty analysis process and results. Lastly, section VI summarizes the results and prescribes future analysis.

II. Thrust Reverser Model

Before the construction of the thrust reverser model, a literature survey was conducted to collect information on thrust reverser types and methods for modeling thrust reversers. Thrust reverser types can be broken down into two primary categories: cold stream (bypass) and hot stream. Bypass thrust reversers only deflect the bypass stream to generate reverse thrust (the core, hot stream, will still produce forward thrust). The hot-stream type thrust reverser uses buckets (or targets) at the back end of the engine to redirect all the exhaust from the engine. The model is constructed to analyze both types of thrust reversers; however, in this paper the model is demonstrated for the hot-stream thrust reverser.

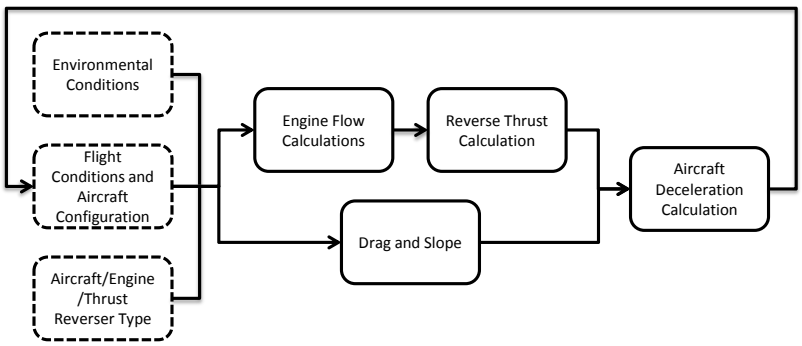

Figure 1. Thrust reverser model overview.

A variety of methods are available for calculating thrust reverser performance ranging from low-fidelity thrust reverser efficiency models to high-fidelity CFD simulations. For this analysis a volume approach was selected, which calculates mass flow rate through the system along with inlet and nozzle velocities. This approach provided the appropriate balance of fidelity and computational time needed for this study.

The thrust reverser model was constructed using MATLAB®/Simulink®[5]. Simulink was the chosen platform because of its inherent ability to model time-based systems. An overview of the model is shown in Fig. 1. In the figure, the inputs for the model are represented in the boxes with dashed lines. All other solid outlined boxes represent modules performing sets of the calculations to derive the aircraft deceleration. Most of the modules contribute to the reverse thrust calculation; however, the model also calculates the effect of drag and runway slope. The other stopping forces were included in the model for validation purposes only.

Table 1. Model Inputs.

Input Module	Variables
Environmental Conditions	• Air pressure • Air temperature • Air humidity
Flight Conditions and Aircraft Configuration	• Ground speed • Air speed • Pitch angle • Spoiler angle • Engine fan speed • Aircraft landing weight • Operating line
Aircraft/Engine Configuration	• Aircraft type • Engine type • Thrust reverser type

The data does not contain a measurement of reverse thrust; therefore, the model was validated based on aircraft deceleration and velocity measurements, which requires capturing all forces acting on the aircraft. Once all the forces were calculated, the aircraft deceleration rate and velocity were computed. The remainder of this section will explain each module shown in Fig. 1 in more detail.

A. Model Inputs

Three categories of inputs are shown in Table 1 along with their associated variables: environmental conditions; flight conditions and aircraft configuration; and aircraft/engine. The environmental conditions required for the calculations can be captured using onboard sensors or weather data. The flight conditions and aircraft configuration parameter are primarily available from the flight data or are iteratively calculated in the model. The only parameter that cannot be directly assessed using flight data or model feedback is the operating line for the engine fan and compressor map. This value is dependent on engine control, engine degradation, and inlet distortion and, therefore, is estimated with a large amount of uncertainty.

The aircraft/engine/thrust reverser type defines many factors in the model. For example, the aircraft type dictates lift and drag coefficients, wing area, aspect ratio, sweep angle, and flap area/span. The engine type determines engine fan map scaling and bypass ratio. The thrust reverser type defines whether only the bypass or the bypass and core flows are used for reverser thrust. In addition, the type of reverser (cascade, pivoting blocker door, bucket, etc.) determines thrust reverser area and efficiency. The information available in the public domain for the variables required for this set is often limited. Estimates can often be made based on the class of aircraft, but the error ranges are relatively high.

B. Engine Station Calculations

The engine station calculation module determines the instaneous total pressure and total temperature throughout the engine. The engine station designations are shown in Fig. 2.

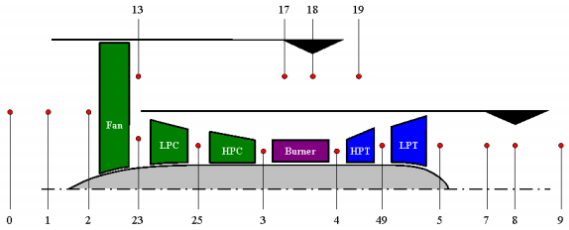

Figure 2. Engine station designations.

The first step in the module determines the pressure and temperature of the air at the inlet of the engine[6]:

$$T_{02} = T_a\left(1 + \frac{\gamma_a - 1}{2} M_a^2\right) \tag{1}$$

$$p_{02} = p_a\left[1 + \eta_d\left(\frac{T_{02}}{T_a} - 1\right)\right]^{\frac{\gamma_d}{\gamma_d - 1}} \tag{2}$$

Also at this stage, air density is calculated based upon ambient temperature, ambient pressure, and relative humidity:

$$\rho_a = \frac{0.028964(p_a - p_v) + 0.018016 * \emptyset\, p_{sat} M_v}{RT} \tag{3}$$

where:

$$p_{sat} = 100\left(6.1078 * 10^{\frac{7.5T}{T+237.3}}\right) \tag{4}$$

To perform the reverser thrust calculation, mass flow rate through the engine and flow velocities at the inlet and nozzle must be known. One method of calculating mass flow rate and pressure ratio is using fan/compressor maps. An example fan map provided by Georgia Tech ASDL is shown in Fig. 3. The fan map provides corrected mass flow rate, fan pressure ratio, and adiabatic efficiency given that engine speed and operating line are known. The blue (somewhat horizontal) lines are the speed lines. These lines are listed as %N1, which can be collected from the aircraft onboard sensors.The operating lines are the black (somewhat vertical) lines in Fig. 3. Typically, the engine is designed to operate in a portion of the map with high efficiency and a generous stall margin (the distance between the actual operating line and the 1.0 R-line); however, engine degradation over time and inlet distortion can cause a reduction in stall margin and has an effect on the operation of the engine.

The actual mass flow rate needed for the thrust calculation is calculated using the fan map, bypass ratio of the engine, and flow temperature and pressure corrections . The pressure ratio calculated from the fan map is used to initiate the engine temperature and pressure calculations, which are needed to calculate nozzle exit velocity.

The bypass (Eq.5) and core (Eq.6) exit velocities are calculated as:

$$\left(\frac{u_8}{u_0}\right)^2 = \frac{\frac{T_{08}}{T_a} - 1}{\frac{T_{08}}{T_{02}} - 1} \quad (5)$$

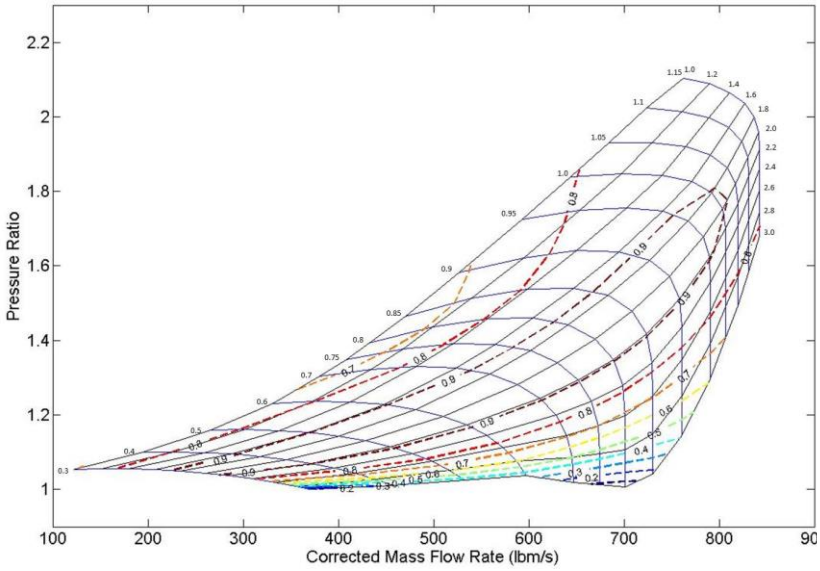

Figure 3. Notional fan map.

$$u_e = \sqrt{2\eta_n \frac{\gamma_n}{\gamma_n - 1} RT_{05}\left[1 - \left(\frac{p_7}{p_{05}}\right)^{\frac{\gamma_n - 1}{\gamma_n}}\right]} \quad (6)$$

The temperatures and pressures are calculated for each engine station from the inlet to the bypass nozzle and core nozzle. See Hill, Ref. 6, for detailed engine station calculation formulas.

C. Reverse Thrust Calculation

After the engine station calculations are performed, a control volume analysis is used for the reverse thrust calculation. A schematic of the control volume is shown in Fig. 4. The analysis is slightly different between a hot-stream and cold-stream thrust reverser. If a hot-stream thrust reverser is used, both the bypass and core flows are deflected to generate reverser thrust. In this case, reverser thrust is calculated as:

$$F_{TR,x} = -\dot{m}_o u_e \cos\beta - \dot{m}_o u_o \quad (7)$$

If only the bypass flow is reversed, the core flow will still generate forward thrust; therefore, the reverse thrust is calculated as:

$$F_x = -\dot{m}_B u_8 \cos\beta - \dot{m}_0 u_o + \dot{m}_C u_7 \quad (8)$$

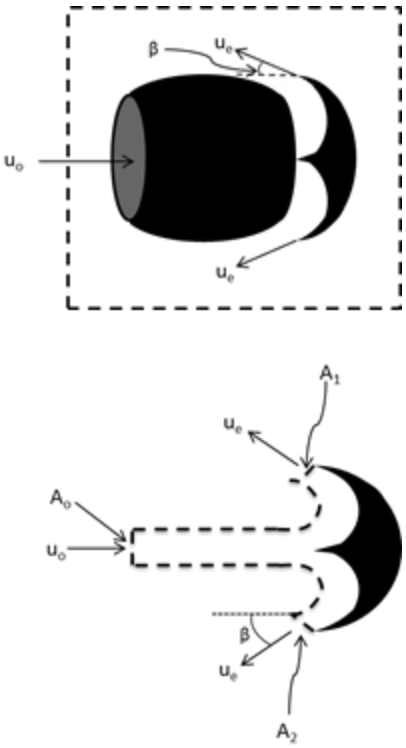

Figure 4. Thrust reverser control volume.

E. Drag and Slope

The other deceleration forces module calculates aerodynamic drag and the effect of runway slope on the aircraft. This module is needed to complete the validation task outlined in section IV. Braking is ignored because little or no braking was applied when the data was collected.

The aerodynamic drag is calculated as:

$$D = \frac{1}{2}\rho V^2 S C_D \tag{9}$$

The drag coefficient consists of several parts: zero-lift drag (C_{D0}), induced drag (KC_L^2), spoiler drag (C_{Ds}), and flap drag (C_{Df})[7]. The zero-lift drag and induced drag was estimated based on published estimates for a business jet in academic texts:

$$C_D = C_{D0} + \frac{C_L^2}{\pi e AR} + C_{D_S} + C_{Df} \tag{10}$$

$$C_{D_S} = \frac{1.9 \sin(\delta_S)\, S_s}{S} \tag{11}$$

$$C_L = C_{L_C} + \Delta C_{L_{HLD}} + \Delta C_{L_S} \tag{12}$$

$$C_{L_S} \approx -C_{L_C} \frac{b_s}{b} \tag{13}$$

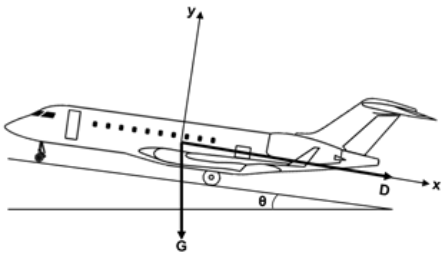

Figure 5. Drag and gravity forces.

In all calculations, the aircraft is used as a frame of reference, meaning the x-axis is aligned with the fuselage of the aircraft and not necessarily with the ground. The reference frame is shown in Fig. 5. If the aircraft is on a runway with a non-zero gradient, the effect of gravity must be considered:

$$F_{g,x} = mgsin(\theta) \tag{14}$$

F. Deceleration Calculation

As shown in Fig. 1, the final step in the algorithm is to calculate the aircraft deceleration. After all forces have been estimated, aircraft deceleration and velocity are calculated using Eq. (15), assuming no braking is used. The calculated acceleration provides insight into how the total forces are affecting the aircraft. The velocity calculation provides an intuive understanding of the deceleration of the aircraft. The aircraft deceleration module uses the output of the thrust reverser module and the other deceleration forces module to calculate the speed of the aircraft. Using Newton's second law of motion:

$$v = -\int \frac{F_{TR,x} + D + F_G}{m}\, dt \tag{15}$$

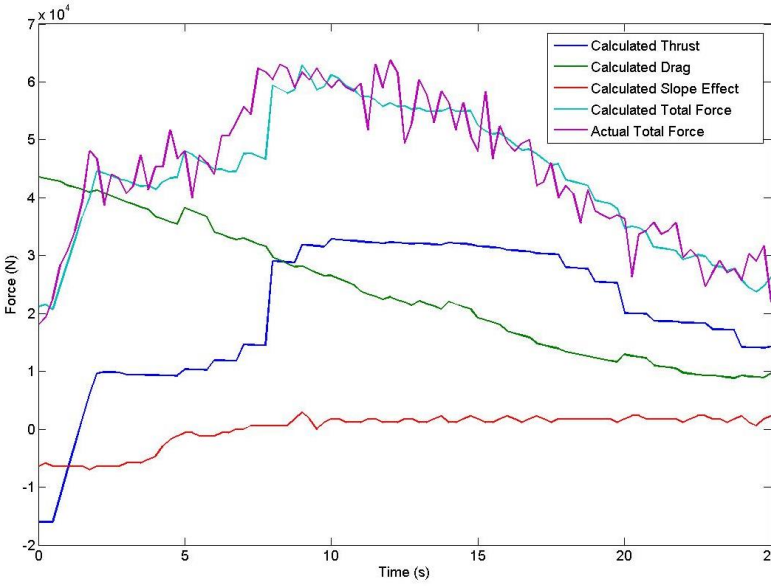

Figure 6. Example model output

III. Model Verification and Validation

The next step in the process was to verify and validate the thrust reverser model. First, the trends of each deceleration force were evaluated. This was accomplished by comparing the model results to the typical aircraft deceleration forces shown in FSF ALAR[8].

The primary output of the model is the forces acting on the aircraft during the landing roll. The forces are calculated in the reference frame of the aircraft with the x-axis oriented such that positive forces act in the opposite direction of the aircraft's velocity vector. The forces that are calculated by the model are: aerodynamic drag, gravity, and reverse thrust (braking is ignored in this model). Aircraft acceleration, velocity, and distance traveled can be calculated from these forces.

An example of the model output is shown in Fig. 6. The model shows the forces on the aircraft for 25 seconds of the landing roll. At the beginning of the simulation, aerodynamic drag is the primary stopping force on the aircraft. At this point, the thrust reversers have not fully deployed, so the engines are creating forward thrust (therefore, a negative force value is shown because the x-axis is oriented toward the rear of the aircraft). Furthermore, because the aircraft has some pitch (and the aircraft is used as a frame of reference), some force due to gravity is translated into the x-axis.

Throughout the landing roll, aerodynamic drag is constantly decreasing because the aircraft is slowing. At approximately the 3-second mark, the engines are in reverse thrust configuration and are starting to spool-up. At approximately 9 seconds, the maximum %N1 is reached, which results in the maximum reverse thrust. At this point %N1 can no longer be increased and the amount of reverse thrust generated begins to reduce because the speed of the aircraft is decreasing.

Table 2. Modeling Error

Set	Maximum magnitude of velocity error (m/s)	Maximum percent velocity error	Maximum magnitude of acceleration error (m/s^2)	Maximum percent acceleration error
1	1.27	3.87	0.18	14.64
2	0.86	2.49	0.19	14.08
3	0.84	2.67	0.35	16.63
4	1.48	5.00	0.22	17.16
5	1.89	5.83	0.28	28.31
6	1.15	4.55	0.30	38.78
7	0.36	0.83	0.59	43.92
8	1.33	3.94	0.36	19.55

To validate the model, data was collected using the FAA's Global 5000 aircraft. Eight test flights occurred on dry runways. The pilot primarily used thrust reversers to slow the aircraft at high speeds, and then braking was added once required for a safe stop. This process was used to isolate the drag and reverse thrust forces. The following parameters were collected at a rate of 4 Hz from the aircraft quick-access recorder (QAR):

- Acceleration (horizontal and vertical)
- Airspeed
- Groundspeed
- Pitch angle
- %N1
- EPR

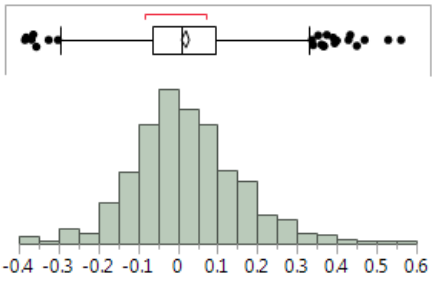

Figure 7. Acceleration error.

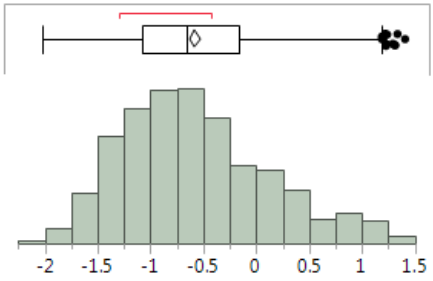

Figure 8. Velocity error.

To validate the model, the longitudinal acceleration computed by the model is compared to the longitudinal acceleration data from the QAR. The model error with respect to the data from 8 test flights is shown in Table 2. For the majority of the data points, the velocity error for the model was held under 5%, and in most cases the acceleration error was less than 30%.

The velocity and acceleration error distributions are shown in Fig.7 and Fig. 8. The mean of the velocity error was -0.58 m/s, suggesting a model bias. Possible sources of bias include not considering rolling resistance or aircraft braking or the bias could be a result of inaccuracies in the model. The mean acceleration error was 0.019 m/s^2 with a standard deviation of 0.133 m/s^2.

Along with validating the model, the distributions shown in Fig. 7 and Fig. 8 were important in defining the expected error from the model. The model error will be analyzed in conjunction with the expected error on the parameter estimates. This analysis will provide some insight into the sources of the model error.

The second part of the validation process was to perform a Matched Pairs analysis using JMP[9]. The Matched Pairs analysis uses a student's t-test to test the null hypothesis that the average difference between two data sets (in this case the actual acceleration of the aircraft and the acceleration calculated by the model) is zero. A 95% confidence interval was used. The results of the matched pairs analysis for the hot-stream thrust reverser are shown in Fig. 9. The plot on the left shows the results for flight 7 and the results on the right are for flight 5 (refer to Table 2; the largest amount of bias was for flight 5).

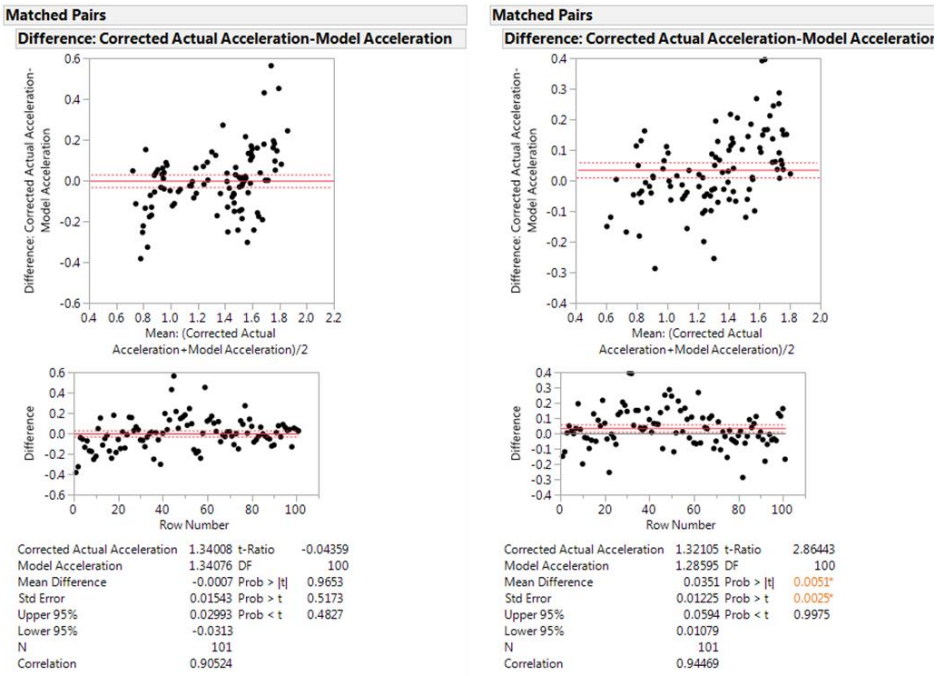

Figure 9. Matched pairs analysis.

IV. Sensitivity Analysis

The primary goal of the sensitivity analysis was to determine which variables have the largest relative influence on predicting the thrust reverser performance. The software tool JMP was used to execute this analysis. The first step was to perform a design of experiments (DOE) to explore the design space. Because a computer model was being assessed, a space-filling design was chosen. The factors considered are listed in Table 3.

Table 3. Sensitivity analysis factors

Factor	Min	Max
Air Temperature	238K	315K
Air Pressure	83000 Pa	102000 Pa
Ejection Angle	30 deg	45 deg
Aircraft Speed	30 m/s	70 m/s
Combustion Temperature	1300K	1700K
Compression Ratio	20	25
Compresor Efficiency	0.96	0.99
Nozzle Efficiency	0.96	0.99
R-line	1.2	2.0

Using the factor settings produced by JMP's DOE, the thrust reverser simulation was repeated 90 times and the model output was collected. (%N1 was set at 0.7.)The data was saved in JMP and a model was fit to the data. The first step was to use a screening process to determine which variables were driving the response and needed to be included in the model. This is a filtering technique used to reduce the total number of variables in the model. Next, a second-order response surface equation (RSE) was fit to the data using the standard least squares estimation method. The model was produced with an R^2 value of 0.9990 and $R^2_{adjusted}$ of 0.9986. A Pareto plot demonstrating the relative importance of each factor is shown in Fig. 10.

The results show that the hot-stream thrust reverser is highly sensitive to ambient temperature. The reason for this can be determined by assessing the effect of ambient temperature on the bypass and core streams. As

temperature increases, the thrust produced by both streams will decrease; however, the change in thrust by the core is more significant than the change in thrust by the bypass stream. For example, an increase of 25K in ambient temperature will cause approximately a 21% decrease in bypass thrust and will cause approximately a 19% reduction in core thrust. The compounded reduction of thrust from both the bypass and core streams causes the net thrust to decrease by approximately 19.5%; therefore, calculated reverse thrust is highly sensitive to ambient temperature.

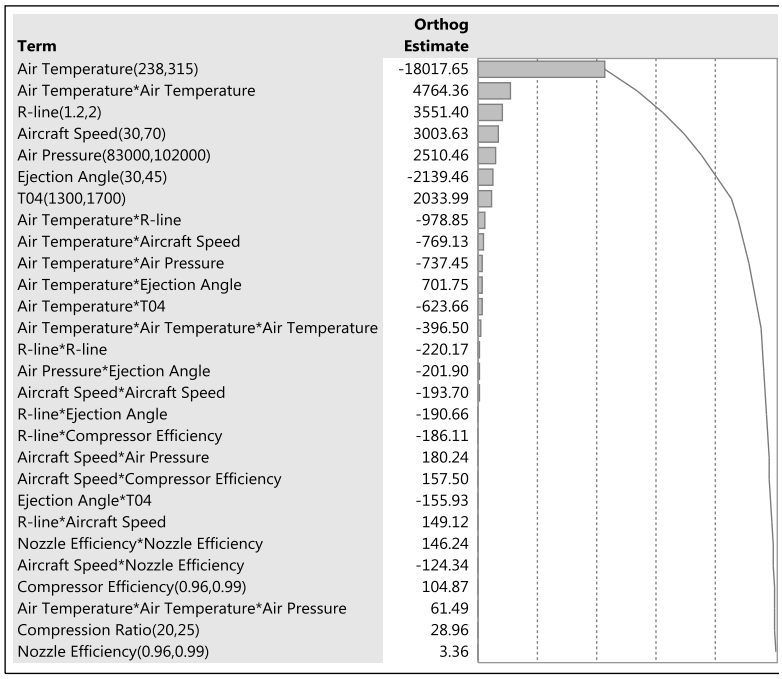

Figure 10. Pareto plot of factors.

Along with air temperature, the operating line, air pressure, and ejection angle have a significant effect on the reverse thrust produced by the hot-stream thrust reverser. Air temperature and air pressure can be estimated with a high degree of accuracy using weather data. An experiment was conducted to assess the effect of air density on reverse thrust, and the results are shown in Fig. 11.

Conversely, the operating line and ejection angle could be significant sources of error. The engine operating line is dependent on a number of factors including engine design, engine control algorithms, engine degradation, and

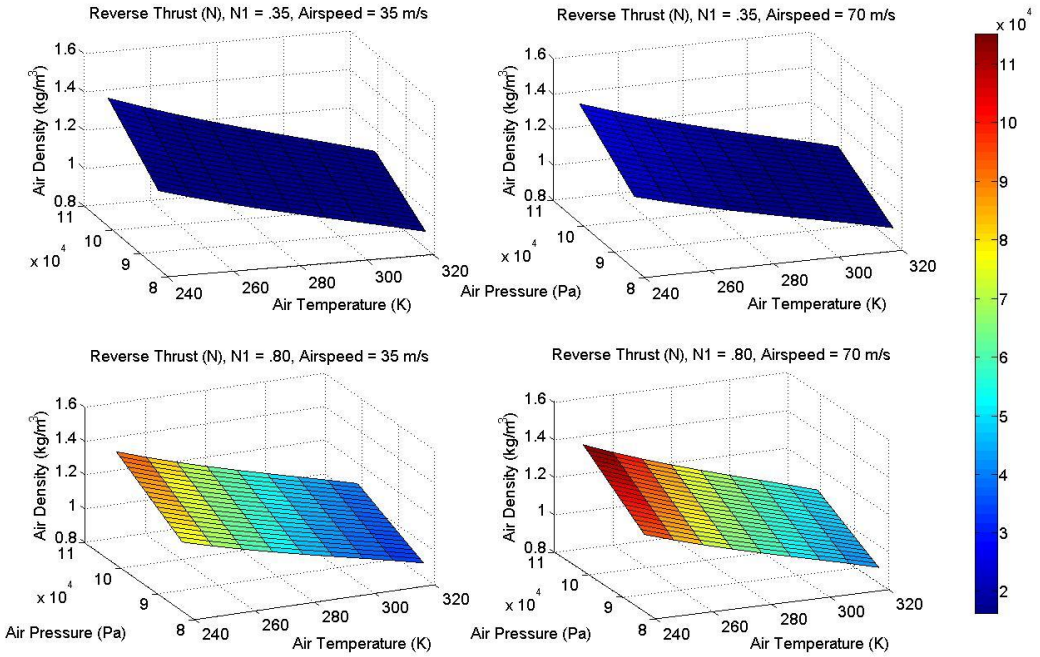

Figure 11. Effect of air densitiy on hot-stream thrust reversers

inlet distortion. Typically, the ejection angle of a hot-stream bucket thrust reverser can be determined by measuring the angle of the buckets (unlike a cascade thrust reverser, which can have hundreds of vanes at a variety of angles).

V. Uncertainty Analysis

The final step in the analysis was to determine the uncertainty in the reverse thrust calculation given the uncertainty in the input parameters. This task was accomplished by developing a worst-case scenario on a standard day; that is, creating uncertainty model inputs that represent the largest amount of uncertainty that should be encountered at standard temperature and pressure. First, a literature survey was conducted to determine the expected accuracy of the input parameters (the only parameters that were considered were those that the sensitivity analysis showed to be important for the response). The references used and uncertainty estimates are summarized in Table 4.

The uncertainty of airspeed, %N1, air pressure, and air temperature is determined by the accuracy of instrumentation onboard the aircraft. According to 14 CFR Part 121 appendix B and appendix M, the required accuracy of flight recorder parameters are: ±5% for airspeed, ±2°C for outside air temperature, and ±100–700 ft for pressure altitude (approximately ±4-26 hPa for outside air pressure)[17]. A typical standard deviation of %N1 is 0.25% according to Ganguli.[10] The accuracy of operating line, ejection angle, and combustion temperature (T04) is limited by the information available in the public domain. The range for the operating line was set based on reasonable operating lines found in the fan map. Operating lines outside of the range listed in Table 4 would either put the fan on the verge of stall or result in unacceptably low efficiency. The range for ejection angle was set by surveying available target-type thrust reverser design information. The angles of the buckets all fell within the range listed in Table 4. No specific information could be found on the combustion temperature of the BR700 engine; therefore, a relatively large band of uncertainty was set for the T04 estimate.

Table 4. Uncertainty ranges and distributions.

Parameter	Uncertainty	Distribution
Airspeed[15]	±5%	$N(60,1.5)$
Air Pressure[15]	±4-26 hPa	$N(101325, 1300)$
Air Temperature[15]	±2°C	$N(273,1)$
%N1[10]	$\sigma = 0.25\%$	$N(0.7, 0.0025)$
Operating Line	1.4-2.4	$N(1.9.0.1)$
Ejection Angle[11-14]	45 – 55	$U(44,52)$
T04	± 200K	$N(1500,100)$

A Monte Carlo simulation was used to determine how the uncertainties in the input parameters propagate to the reverse thrust calculation. The distributions defined in the third column of Table 4 were used for the random sampling of the model input parameters, and the surrogate model created for the sensitivity analysis was used for the calculations. A normal distribution was used for the measured parameters (airspeed, air temperature, and air pressure). To define the distribution, an actual (or true) value for each parameter was set and then the standard deviation was defined to produce a distribution with an error range reflective of the values shown in Table 4. The actual/true values for airspeed, air temperature, and air pressure are 60 m/s, 273K, and 101,325 Pa, respectively. The true values were selected to represent the reverse thrust at high speed at standard temperature and pressure.

The remaining parameters are dependent on engine and thrust reverser design and their associated error distributions are representative of model error and not measurement error. The modeling error is caused by lack of public data on the engine and thrust reverser design. A normal distribution was chosen for the operating line because the actual operation point of the engine should fluctuate around the high efficiency point of the fan map with descreasing probability at the tails. The actual operating line is dependent on engine design, engine control, engine degradation, and inlet distortion, so the distribution was set such that the mean was the optimal operating point and the standard deviation was selected such that the distribution would cover the range found in the second column of Table 4. The expected combustion temperature was selected to be 1500K (a typical combustion temperature for turbofan engines). A normal distribution was used to define the uncertainty with a mean of 1500K and a standard deviation of 100K. With a standard deviation of 100K, it is assumed that all realistic temperatures for T04 are covered. A uniform distribution was used for the ejection angle because the likelihood of the true value is the same throughout the defined range.

After the input distributions were defined, a 10,000 run Monte Carlo simulation was performed; that is, each distribution was sampled 10,000 times, the model was run 10,000 times, and 10,000 reverse thrust responses were calculated. A histogram of the 10,000 reverse thrust values calculated is shown in Fig. 12. The figure shows a normal distribution with a mean of 65,278 N of reverse thrust. Approximately 50% of the distribution falls within ±2.5% of the median, and approximately 90% of the distribution falls within ±10% of the median. Over the first 25

seconds of the landing roll, a 10% error in reverse thrust creates an approximate 12 meter error on the distance traveled by the aircraft. For an aircraft that touches down at approximately 120 knots, this equates to approximately 1% of the total distance traveled by the aircraft over the 25 seconds analyzed.

Given the uncertainty distributions of the input variables, the uncertainty response is most sensitive to the operating line because of the large spread of the uncertainty distribution and its direct impact on engine pass flow rate and fan pressure ratio. If a more accurate estimate of the operating line is available, the uncertainty of the response can be significantly reduced. T04 had the second-largest impact on the variability in the reverse thrust response. The uncertainty contributed by T04 could be reduced if the expected combustion temperature for the engine is known. The %N1, air temperature, airspeed, and air pressure all have a similar impact on the uncertainty response of the reverser thrust calculation. It is unlikely that the uncertainty associated with %N1, air temperature, air pressure, and airspeed can be significantly reduced because the uncertainty associated with those parameters is measurement uncertainty and not model uncertainty. Ejection angle uncertainty had the least effect on the thrust reverse response; therefore, the lack of detailed information on the angle of the buckets for the thrust reverser does not have a large detrimental effect on the model's ability to predict reverse thrust.

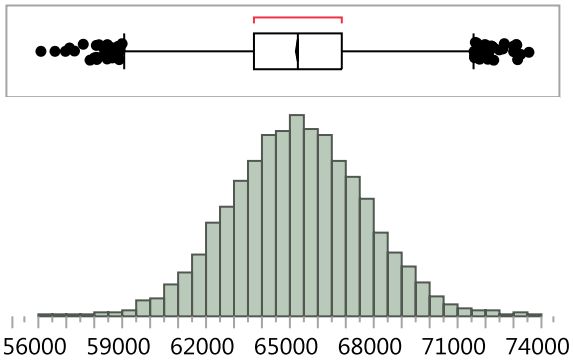

Figure 12. Reverse thrust histogram.

VI. Conclusion

In summary, this paper provided a methodology for quantifying the uncertainty of calculating reverser thrust using in situ data. For this analysis, a thrust reverser model was developed in MATLAB/Simulink that only uses publically available information. By using flight data collected by the FAA's Global 5000 aircraft, it was shown that the model could consistently predict the acceleration of the aircraft within 30% and the aircraft velocity within 5% throughout the landing roll.

To narrow the number of parameters to be included in the uncertainty analysis, a sensitivity analysis was performed to determine which variables in the model drive the reverser thrust response. The analysis determined that the most important factors in the model are air temperature, operating line, airspeed, air pressure, ejection angle, and combustion temperature (T04).

To perform the uncertainty analysis, the expected measurement and model errors were quantified and a Monte Carlo simulation was performed. The analysis showed that 95% of the results fell within ±10% of the mean thrust value. A 10% change in thrust equates to an approximate 1% error in the calculated distance traveled by the aircraft during the landing roll. Two of the driving factors of uncertainty are the engine operating line and combustion temperature. Both values had large uncertainty distributions due to the lack of information published in the public domain. Therefore, it is reasonable to expect that the accuracy of the model could be improved by focusing on reducing the uncertainty associated with those two parameters.

The analysis process demonstrated in this study provides a tool in determining not only the uncertainity of reverse thrust calculation but also the validity of a runway friction assessment method using onboard aircraft data. The uncertainty of all calculated forces on the aircraft must be quantified to allow further evaluation of which calculations need to be improved, if any, to achieve an operationally viable method for assessing runway slipperiness.

Acknowledgments

The authors wish to thank Paul Giesman, at the FAA Transport Airplane Directorate, for providing his input and expertise on the aircraft-based runway friction assessment method. They would also like to thank the pilots and engineers at the FAA William J. Hughes Technical Center, who contributed to the experiment, and especially thank Timothy Hogan for his administrative support, Fred Karl for arranging and conducting the flight tests, and Diane Bansback for pre-processing the flight data for analysis.

References

[1]Boeing, "Statistical Summary of Commercial Jet Airplane Accidents: Worldwide Operations," Aviation Safety, Seattle, 2013.

[2]Flight Safety Foundation, "Reducing the Risk of Runway Excursions," Runway Safety Initiative, 2009.

[3] van Es, G. W.H., van der Geest, J., Cheng, A., and Stimson, D., "Aircraft Performance in Slippery Runway Conditions: A Simulation Study of the Accuracy and Limitations of Real-time Runway Friction Estimation Based on Airplane Onboard Data," DOT/FAA/TC-14/32, January 2015

[4] Mckay, Gary E., "Calculation of Dynamic Tire Forces from Aircraft Instrumentation Data," Tire Science and Technology, TSTCA, Vol. 38, No. 3, July-September 2010, pp. 182-193.

[5]MATLAB/Simulink, Software Package, Ver. R2013b, Mathworks, Natick, MA, 2013.

[6]Hill, P., and Peterson, C., *Mechanics and Thermodynamics of Propulsion*, 2nd ed., Addison-Wesley Publishing Company, Inc., Reading, 1992.

[7]Sadraey, M., *Aircraft Performance Analysis*, VDM Verlag Dr. Müller, Saarbrucken, 2011, Chap. 16.

[8]Flight Safety Foundation, "ALAR Tool Kit: FSF ALAR Briefing Note 8.4 – Braking Devices," *Flight Safety Digest*, August – November 2000, pp. 173-177, Alexandrai, VA, 2000.

[9]JMP, Software Package, Ver. 12.1, SAS Institute, Inc., Cary, NC, 2015.

[10]Ganguli, R., *Gas Turbine Diagnostics: Signal Processing and Fault Isolation*, Taylor & Francis Group, Boca Raton, 2013.

[11]Santin, M. A., Barbosa, J. R., Bontempo, L., Silva, F., Jesus, A. B., Trapp, L. G., and Oliveira, G. L., "Overview on Thrust Reverser Design," *18th International Congress of Mechanical Engineering* , Ouro Preto, 2005.

[12]Asbury, S. C., and Yetter, J. A., "Static Performance of Six Innovative Thrust Reverser Concepts for Subsonic Transport Applications," NASA/TM-2000-210300, Hampton, 2000.

[13]Dietrich, D. A., and Luidens, R.W., "Experimental performance of cascade thrust reversers at forward velocity," NASA-TM-X-2665, Cleveland, 1973.

[14]Rudolph, "Jet thrust reverser". USA Patent US4183478 A, 15 January 1980.

[15]Aeronautics and Space, 14 CFR Part 121§ Appendix B and D